The Effect of Multiprinciple Line Protection on Dependability and Security

Jeff Roberts, Demetrios Tziouvaras, Gabriel Benmouyal, and Hector J. Altuve
Schweitzer Engineering Laboratories, Inc.

Published in
Line Current Differential Protection: A Collection of Technical Papers Representing Modern Solutions, 2014

Previously presented at the
3rd Beijing International Conference on Power Transmission and Distribution Technology, November 2001,
55th Annual Georgia Tech Protective Relaying Conference, May 2001,
54th Annual Conference for Protective Relay Engineers, April 2001,
and V Simposio Iberoamericano Sobre Proteccion de Sistemas Electricos de Potencia, November 2000

Originally presented at the
Southern African Power System Protection Conference, November 2000

THE EFFECT OF MULTIPRINCIPLE LINE PROTECTION ON DEPENDABILITY AND SECURITY

Jeff Roberts, Demetrios Tziouvaras, Gabriel Benmouyal, and Hector J. Altuve
Schweitzer Engineering Laboratories, Inc.
Pullman, WA USA

ABSTRACT

Using multiple relaying principles for each line is a common requirement for high-voltage transmission line protection. The philosophy behind this requirement is based on the remote likelihood of one particular fault being undetected by at least two different detection methods. We explore whether using two different relaying principles really delivers the desired redundancy and whether the same factors influence the fault resistance coverage. Many different relaying principles are suitable for pilot protection, but a natural combination of protection elements for these schemes is distance (21), directional (32), and line differential (87L). This paper explores the technical performance issues of applying these relays together from the perspective of dependability and sensitivity. Issues we discuss for 21, 32, and 87L elements and the associated schemes include:

- Limits of fault resistance (R_F) coverage
- CT saturation effect on sensitivity of directional-comparison and 87L schemes
- Communications channel delays

Our analysis includes three-terminal line applications and the special case of fault current outfeed from one terminal for internal ground faults.

We discuss different line current differential characteristics and how they affect dependability and security. We review how to plot these characteristics on the alpha plane (real and imaginary components of the ratio I_{REMOTE} / I_{LOCAL}) as a means of better understanding relay performance during CT saturation and extreme communications channel asymmetry.

INTRODUCTION

Pilot protection provides high-speed, simultaneous fault clearing for faults anywhere along the protected transmission line. From an IEEE survey [1], the most widely used pilot protection system is directional comparison. This 1988 report stated that about 80 percent of the critical lines in 116 utilities use directional-comparison protection. The main reasons for this wide acceptance are the limited channel requirements and the inherent redundancy and backup of directional-comparison systems. However, directional-comparison systems require voltage information. Compared with conventional current-only schemes, these schemes deliver good ground fault resistive coverage.

Phase-comparison and current-differential systems only use current information but require a reliable communications channel. Current-only systems exhibit good performance in complex protection problems, such as evolving, intercircuit, and cross-country faults, mutual induction, power swings, and series impedance unbalance. Current-only systems are also a good solution for series-compensated, three-terminal, and short transmission lines (directional-comparison

schemes are equally applicable to electrically short lines if the relays are properly polarized). Modern digital communications channels [2], [3] fulfill the requirements of current-only pilot protection systems.

Phase-comparison systems compare the phase of the currents at all line terminals. Early systems used a composite sequence network to form a single-phase voltage for phase comparison. Modern digital communications channels permit implementation of segregated phase comparison systems that provide faulted phase identification and enhance the protection response to complex faults.

Traditional phase-comparison systems fail to detect higher impedance internal faults with outfeed. Offset keying [4] is an enhancement to phase comparison that adds magnitude information to the phase comparison process in order to accommodate outfeed. However, offset-keying phase-comparison systems have sensitivity limitations for faults with low fault current contributions at all line terminals (i.e. high impedance faults).

A basic limitation of traditional line current differential systems is that the user must select a slope (or slopes) appropriate to the expected current transformer saturation and maximum channel asymmetry. This slope setting defines a relay characteristic with a given tolerance to channel time-delay asymmetry and CT saturation but also limits the relay sensitivity to internal faults during outfeed. Thus, relays using settable slope characteristics cannot individually address current transformer saturation, channel asymmetry, outfeed, and other problems; one setting must suffice for all. Later in this paper we show a new characteristic that allows you to address each problem and still maintain good sensitivity.

Charge comparison [5] is an alternate form of current-differential line protection. This type of protection reduces the communications channel requirements. Charge-comparison systems provide higher tolerance to channel asymmetry and outfeed than traditional current-differential systems. However, the required zero-crossing detection introduces a half-cycle latency that penalizes speed and introduces additional time delay for internal faults with full dc offset. External faults with current transformer saturation that affect current zero-crossings may produce relay misoperations.

PILOT PROTECTION OF TRANSMISSION LINES

Pilot protection uses a communications channel or channels to exchange information between the transmission line terminals. Using information from all line terminals, pilot protection provides high-speed simultaneous detection and clearing of phase and ground faults along the protected line.

Traditional pilot protection communications channels include pilot wires, power line carrier, and microwave. Utilities still widely use the latter two channels. Fiber optics emerged in the early 1980s as a new type of communications means for pilot protection [2]. Fiber optics has broad bandwidth and eliminates electrical induction, noise, and electrical insulation problems of traditional channels.

We may classify pilot protection systems as blocking or transfer trip systems. This classification corresponds to the way the local relay uses remote terminal information to generate the tripping signal. Blocking systems do not require the remote signals to trip. Transfer trip systems must receive the remote signals to issue a local tripping signal. Blocking systems tend toward higher

dependability than security: a failure to receive a blocking signal from a remote terminal can result in misoperation for an external fault. These same schemes also achieve higher fault resistance coverage than others for higher impedance faults close to one terminal because they can trip when only one relay senses an in-section fault. Once one terminal has tripped, the remote relay can generally sense the remote fault and trip sequentially. Transfer trip systems tend toward higher security than dependability: a failure to receive a tripping signal can result in a failure to operate for an internal fault. Transfer trip pilot systems are faster than blocking systems, but require additional logic to ensure internal-fault operation when one line terminal is open or weak.

According to the fault detection principle, we may classify pilot protection systems as directional-comparison, phase-comparison, and current-differential systems.

Directional-Comparison Pilot Protection Systems

Figure 1 shows a diagram of a directional-comparison system. This system uses directional and distance elements to discriminate internal from external faults.

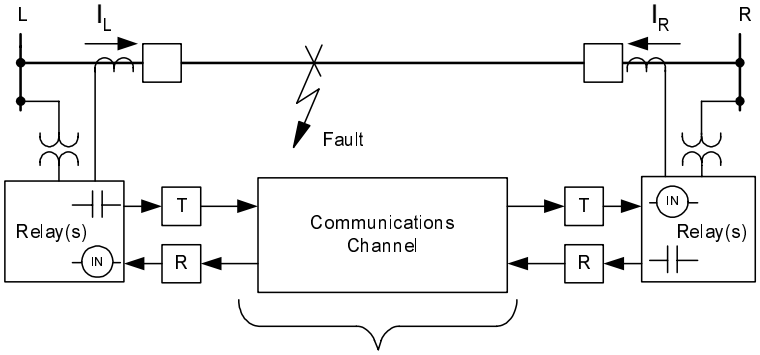

(a) Contact Input/Output Interface to Communications Channel Equipment

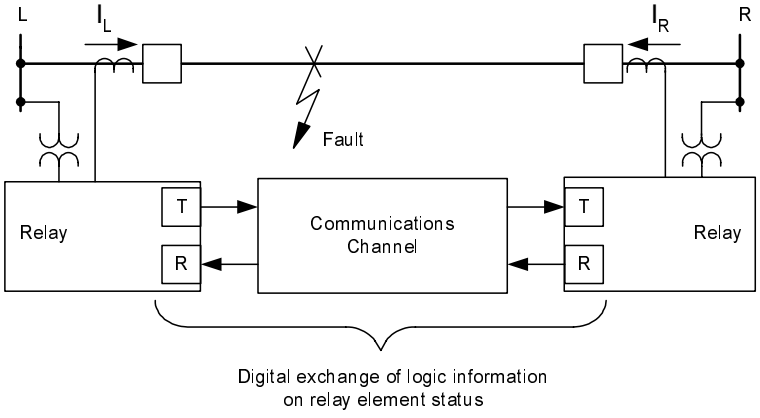

(b) Digital Interface Between Relay and Communications Channel

Figure 1 Schematic Diagram of a Traditional Directional-Comparison System

Relays at all terminals require current and voltage information to determine the fault direction. The protection system uses the communications channel to exchange only logic information

about relay contact status. In the system shown in Figure 1(a), the relay interface to the communications channel equipment is via contact inputs and outputs. The two-state type of information requires very low channel throughput (about 0.8 to 1.2 kHz bandwidth). For these systems, the relay has no information about the channel health. For the system shown in Figure 1(b), the relay interface to the communications channel is digital. With a slight increase in channel bandwidth (to about 3 kHz), the protection system communicates the status of eight digital outputs and eight inputs. These systems communicate up to eight times the information (important for today's trip and control schemes) while simultaneously monitoring the channel health and availability. Channel delay or asymmetry is not critical to these schemes: a delay in receiving the remote signal may delay tripping, but the delay does not affect whether the trip or restrain decision is correct. The inherent redundancy provided by the directional and/or distance elements ensures tripping for internal faults given a channel failure.

Current-Differential Pilot Protection Systems

Digital current differential pilot systems use the communications channel to exchange digital information of the currents at the line terminals. Most of today's systems exchange phasor information. Percentage-differential elements compare an operating current with a restraint current. The operating current, I_{OP}, is the magnitude of the phasor sum of the currents.

$$I_{OP} = \left| \vec{I}_L + \vec{I}_R \right| \tag{1}$$

I_{OP} is proportional to the fault current for internal faults and ideally approaches zero for any other operating conditions.

The most common alternatives for obtaining the restraint current, I_{RT}, are the following:

$$I_{RT} = k\left| \vec{I}_L - \vec{I}_R \right| \tag{2}$$

$$I_{RT} = k\left(\left| \vec{I}_L \right| + \left| \vec{I}_R \right| \right) \tag{3}$$

$$I_{RT} = \text{Max}\left(\left| \vec{I}_L \right|, \left| \vec{I}_R \right| \right) \tag{4}$$

$$I_{RT} = \sqrt{\left| \vec{I}_L \right| \cdot \left| \vec{I}_R \right| \cos\theta} \tag{5}$$

where k is a constant coefficient, usually taken as 1 or 0.5, and θ is the angle between $\vec{I}_L$ and $\vec{I}_R$. Equations (3) and (4) are applicable to differential relays with two or more restraint elements. For example, for a three-terminal line we may use the following quantities:

$$I_{OP} = \left| \vec{I}_X + \vec{I}_Y + \vec{I}_Z \right| \tag{6}$$

$$I_{RT} = k\left(\left| \vec{I}_X \right| + \left| \vec{I}_Y \right| + \left| \vec{I}_Z \right| \right) \tag{7}$$

where $\vec{I}_X$, $\vec{I}_Y$, and $\vec{I}_Z$ are the currents at the line terminals X, Y, and Z respectively. Later we show a method of reducing a three-terminal line to a two-terminal line equivalent. We may define the operation condition of a percentage-differential relay as:

$$I_{OP} \geq KI_{RT} \tag{8}$$

where K is a constant coefficient representing the relay characteristic slope. In order to provide the relay with a minimum pick-up current, K_0, we add the condition:

$$I_{OP} \geq K_0 \tag{9}$$

Figure 2(a) shows the relay operating characteristic resulting from the equality conditions of both Equations (8) and (9). Another possible definition of the differential relay operation condition is:

$$I_{OP} \geq KI_{RT} + K_0 \tag{10}$$

Figure 2(b) shows the relay characteristic corresponding to Equation (10). It is a straight line having a slope K and an intersect K_0 on the ordinate axis. A variable-percentage or dual-slope characteristic (dotted lines in Figure 2(b)) increases relay security.

The differential current is not exactly zero for external faults. The most common causes of false differential current in transmission line differential relays are the following:

- Line-charging current and tapped load
- Channel time-delay compensation errors
- Current transformer saturation

All of these factors serve to reduce the sensitivity of the line current differential scheme sensitivity if the scheme is optimized for security.

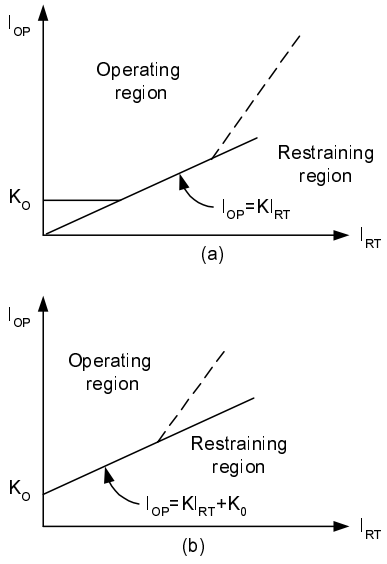

Figure 2 Traditional Differential Relay Operating Characteristics

Line-charging current is significant in cable lines or long overhead lines. The false differential current created by tapped loads may be the result of load current, tapped transformer low-side faults or inrush current in the tapped transformer. We may eliminate the effect of line-charging current and of the load current component of tapped loads using phase differential elements whose minimum pickup is set higher than these "current leaks" from the differential protection scheme. We can only depend upon these higher-set 87L elements in three-phase faults. To detect all unbalanced faults, we can use a much more sensitively set negative-sequence differential

element (later we discuss the disadvantage of using zero-sequence differential elements caused by the effect of CT saturation). We may set these elements much more sensitively because negative-sequence charging current is very low. Channel time-delay compensation errors and CT saturation contribute to false differential current in all types of differential elements. To address these two sources of error we need to carefully design the operating characteristic of the differential element.

Comparing Pilot Protection Systems

We divide pilot protection systems into two groups for discussion purposes. These groups are directional-comparison systems and current-only systems. The latter group includes phase-comparison and current-differential pilot systems. Basic differences between the two general types of pilot systems make them complementary: advantages of one type are drawbacks of the other and vice-versa.

Advantages of Directional-Comparison Pilot Systems

- Channel delay and channel asymmetry requirements are limited
- Inherent remote back-up protection provided by the directional and/or distance elements with suitable timers
- Fault location and fault recording capabilities of both voltage and current provided by most relays with directional or distance elements
- High fault resistance (RF) coverage
- Current transformer (CT) saturation tolerance

References [29] to [31] detail the sensitivity limitations of the directional and distance elements used in these schemes. In summary, these limitations are not set by the relays, but by the power system unbalances and instrument transformer inaccuracies.

Advantages of Current-Only Pilot Systems

- Do not require voltage information (avoiding loss-of-potential problems for close-in faults and blown potential fuses, ferroresonance in VTs and transients in CVTs)
- They are immune to:
  - Zero-sequence mutual induction effects
  - Series impedance unbalance
  - Current reversals and power swings
- Perform well for evolving, intercircuit, and cross-country faults
- Tolerate high line loading
- Depending on the operating characteristic, these systems may handle outfeed

The basic limitations of current-only systems are related to the communications channel (they require a reliable, high-capacity channel) and CT saturation. The channel limitations are rapidly disappearing with modern digital fiber optics. In addition, digital technology permits inclusion of many protection functions in a relay unit. It is then possible to combine a directional-comparison and a current-only pilot system in the same relay. This diversity of operation principles in the same unit enhances the overall scheme performance without a significant cost increase.

CURRENT-RATIO PLANE CHARACTERISTICS OF CURRENT-ONLY SYSTEMS

Let us next evaluate the two dominant factors that affect the sensitivity and security of current-only schemes: channel asymmetry and CT saturation. Current-only line protection systems perform phase or amplitude comparison of quantities derived from the currents at the line terminals. We use a polar current diagram to represent the operation characteristic of phase-comparison systems. A scalar current diagram showing the operating current as a function of the restraint current is the typical way of representing the differential relay operating characteristics.

Relay input signals can have real and imaginary components. The most comprehensive way to represent relay characteristics is to use a complex plane defined by the ratio of the relay input signals [21], [22]. For relays having current and voltage input signals, the complex plane could be represented on an impedance or admittance plane. For relays with only current inputs, the complex plane is a current-ratio plane.

Current-Ratio Plane

We next define a complex term given by the ratio of remote, $\vec{I}_R$, to local, $\vec{I}_L$, currents:

$$\frac{\vec{I}_R}{\vec{I}_L} = a + jb = \vec{r} = re^{j\theta} \tag{11}$$

where:

$$a = \frac{\left|\vec{I}_R\right|}{\left|\vec{I}_L\right|}\cos\theta = r\cos\theta, \quad b = \frac{\left|\vec{I}_R\right|}{\left|\vec{I}_L\right|}\sin\theta = r\sin\theta, \quad r = \sqrt{a^2 + b^2}, \quad \theta = \arctan\frac{b}{a}$$

Equation (11) is the base for the Cartesian—or polar—coordinates versions of the current-ratio plane. Warrington [21], [22] introduced the term alpha-plane to designate the $\vec{I}_R / \vec{I}_L$ plane, and the term beta-plane for the $\vec{I}_L / \vec{I}_R$ plane. Both planes are equivalent in terms of the information they provide.

Current-Differential Relay (87L) Characteristics

Obtain the current-ratio plane characteristic of an 87L having Equation (8) as the operating equation and with a restraint quantity given by (2), with k = 1 for simplicity. Substituting Equations (1) and (2) in Equation (8):

$$\begin{aligned} \left|\vec{I}_L + \vec{I}_R\right| &\geq K\left|\vec{I}_L - \vec{I}_R\right| \\ \left|1 + \frac{\vec{I}_R}{\vec{I}_L}\right| &\geq K\left|1 - \frac{\vec{I}_R}{\vec{I}_L}\right| \end{aligned} \tag{12}$$

Substituting Equation (11) in Equation (12):

$$\left|1 + a + jb\right| \geq K\left|1 - a - jb\right|$$

Expanding the previous equation, we get:

$$a^2 + b^2 + 2\frac{1+K^2}{1-K^2}a + 1 \geq 0 \tag{13}$$

The equality condition in Equation (13) represents the relay threshold operation condition and describes the relay operation characteristic. It is the equation of a circle with a radius, R_c:

$$R_c = \frac{2K}{1-K^2} \tag{14}$$

The location of the circle center in the complex plane is:

$$a_c + jb_c = -\frac{1+K^2}{1-K^2} + j0 \tag{15}$$

Figure 3 shows a family of relay operation characteristics for different values of the slope, K. The operating region is the area out of the circle (Equation (13)), and the restraint region is inside the circle. Note that the –1 + j0 point corresponding to an ideal through-current condition lies inside the relay restraint region.

Table 1 summarizes the characteristics of 87L relays having Equation (8) or (10) as the operating equation, and with different types of restraint quantities (Equations (2) to (5)). Table 1 also includes the characteristic of the unrestrained differential element, which corresponds to $I_{RT} = 0$ in Equation (10).

In general, differential relays described by Equation (8) have circular characteristics (see Table 1). An exception is the frequent case in which the relay restraint quantity is of the type in Equation (3). Figure 4 shows a family of relay characteristics for this case. Note that the value of the slope, K, determines both the size and shape of the relay characteristic. The relay with a restraint quantity of the type in Equation (4) has two different circular characteristics, depending on the relative magnitudes of I_L and I_R.

Differential relays described by Equation (10) do not generally have circular characteristics (see Table 1). The only circular characteristics are those of the unrestrained differential element ($I_{RT} = 0$) and the relay having a restraint quantity of the type in Equation (4) (the characteristic is circular only for $I_L > I_R$). Note that in these two circular characteristics the radius depends on the parameters K and K_0, and the local current magnitude, I_L.

Dual-slope 87L relays may have two different types of operating characteristics in the current-ratio plane. If the first slope characteristic corresponds to Equation (8), the characteristic in the current-ratio plane is a circle (unless the restraint quantity is of the type in Equation (3)). The second slope characteristic has an intersect on the restraint current axis. It is of the type in Equation (10), which gives a noncircular operating characteristic.

Table 1 Differential Relay Characteristics in the Current-Ratio Plane

Operation Equation: IOP	Restraint Quantity: IRT	Type of Characteristic	Center	Radius
KI_{RT}	$\left\|\vec{I}_L - \vec{I}_R\right\|$	Circular	$-\frac{1+K^2}{1-K^2}+j0$	$\frac{2K}{1-K^2}$
	$\left\|\vec{I}_L\right\|+\left\|\vec{I}_R\right\|$	Not Circular	—	—
	$\text{Max}\left(\left\|\vec{I}_L\right\|,\left\|\vec{I}_R\right\|\right)$	$\left\|\vec{I}_L\right\|>\left\|\vec{I}_R\right\|$ Circular	$-1+j0$	K
		$\left\|\vec{I}_L\right\|<\left\|\vec{I}_R\right\|$ Circular	$-\frac{1}{1-K^2}+j0$	$\frac{K}{1-K^2}$
	$\sqrt{\left\|\vec{I}_L\right\|\cdot\left\|\vec{I}_R\right\|\cos\theta}$	Circular	$-\left(1-\frac{K^2}{2}\right)+j0$	$\frac{K}{2}\sqrt{k^2-4}$
$KI_{RT}+K_0$	$I_{RT}=0$	Circular	$-1+j0$	$\sqrt{\frac{K_0}{\left\|\vec{I}_L\right\|}}$
	$\left\|\vec{I}_L - \vec{I}_R\right\|$	Not Circular	—	—
	$\left\|\vec{I}_L\right\|+\left\|\vec{I}_R\right\|$	Not Circular	—	—
	$\text{Max}\left(\left\|\vec{I}_L\right\|,\left\|\vec{I}_R\right\|\right)$	$\left\|\vec{I}_L\right\|>\left\|\vec{I}_R\right\|$ Circular	$-1+j0$	$\sqrt{1+\left(K+\frac{K_0}{\left\|\vec{I}_L\right\|}\right)^2}$
		$\left\|\vec{I}_L\right\|<\left\|\vec{I}_R\right\|$ Not Circular	—	—
	$\sqrt{\left\|\vec{I}_L\right\|\cdot\left\|\vec{I}_R\right\|\cos\theta}$	Not Circular	—	—

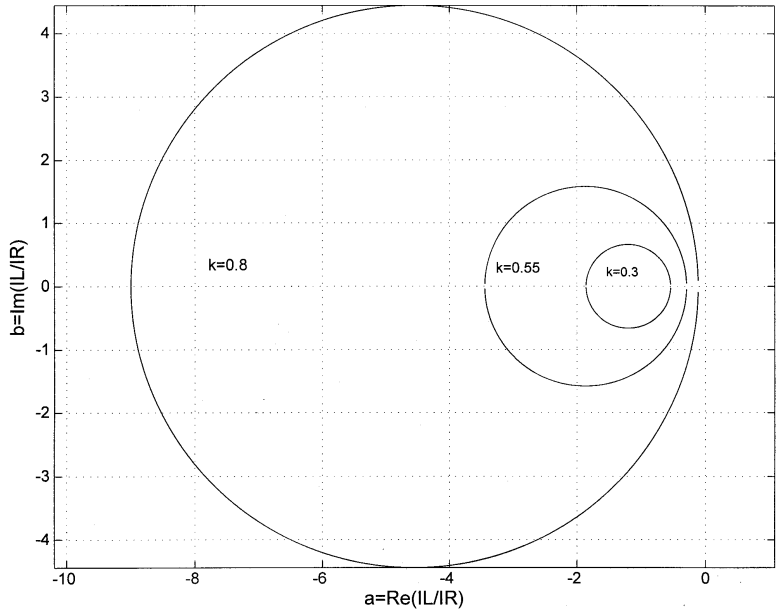

Figure 3 Differential Operating Characteristics Described by Equations (2) and (8)

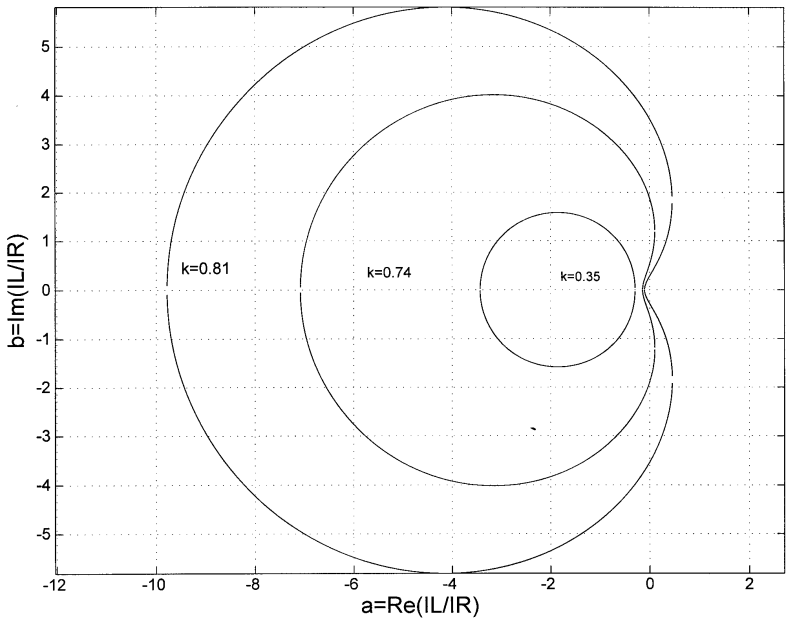

Figure 4 Differential Relay Operating Characteristics Described by Equations (3) and (8)

CURRENT-RATIO TRAJECTORIES

The current-ratio plane is an excellent tool to analyze current-only protection system response to different power system conditions and to channel asymmetry. The method for analyzing relay operation is to superimpose on the same current-ratio plane the relay characteristic and the current-ratio trajectory resulting from the fault or abnormal power system condition. This method is equivalent to analyzing distance relay performance in the impedance plane.

For power-system and protection-scheme steady-state conditions, the current-ratio trajectory reduces to a point. Figure 5 shows current-ratio plane regions for steady-state fault and load conditions. If we disregard all possible sources of errors and any supervisory logic intended to block the phase elements from operating during nonfault conditions, the point representing the system condition falls along the real or a-axis. For ideal through-current conditions (normal loads or external faults), a = –1. For internal faults with infeed from both line ends, a > 0. For internal faults with outfeed at one terminal, a < 0. Note that the relay characteristic should have the point a = –1, in the restraint zone and all faults should lie in the operation zone.

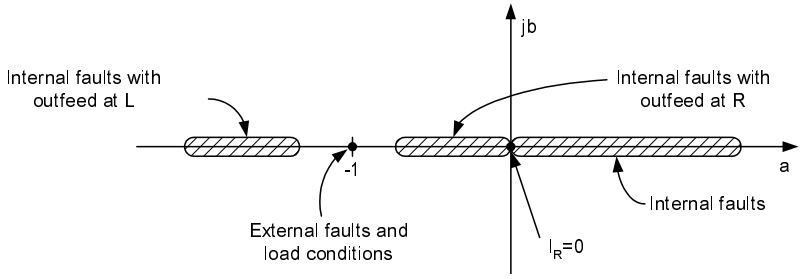

Figure 5 Current-Ratio Plane Regions for Ideal Fault and Load Conditions

System Power Angle and System Impedance NonHomogeneity

For internal faults, the angles of the phase currents $\vec{I}_L$ and $\vec{I}_R$ depend on the angles of the corresponding source voltages and on the angles of the impedances from the corresponding source to the fault point. In general, the currents at both line ends are not exactly in phase for an internal fault. Figure 6 shows the modification of the fault regions when θ varies within ±30° for internal faults. Note that the regions corresponding to load, external faults, and internal faults with outfeed remain unchanged.

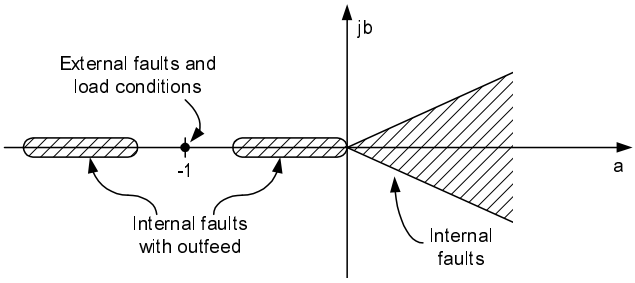

Figure 6 Effects of the System Power Angle and the System Impedance NonHomogeneity

Line-Charging Current

Line-charging current flows into the line at both line terminals and creates a false differential phase current. Figure 7(a) represents the current components that we have in the line for a normal load condition. The currents at both line terminals are:

$$\vec{I}_L = \vec{I}_{LOAD} + \vec{I}_C \text{ and } \vec{I}_R = -\vec{I}_{LOAD} + \vec{I}_C$$

where I_{LOAD} is the load current and I_C is the charging current at each line end. Then:

$$\frac{\vec{I}_R}{\vec{I}_L} = a + jb = \frac{-\vec{I}_{LOAD} + \vec{I}_C}{\vec{I}_{LOAD} + \vec{I}_C} \tag{16}$$

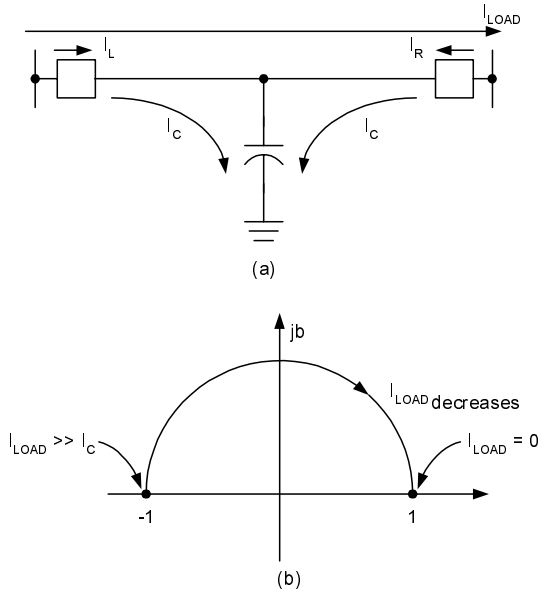

Figure 7 Effect of Line-Charging Current Changes with Magnitude of Load Flow

Figure 7(b) shows the current-ratio locus (Equation (16)) for different values of I_{LOAD}. The trajectory is not generally circular. Note that for small load currents the current-ratio value lies in the right semi-plane. The only way to avoid relay misoperation is to set the relay minimum pickup current greater than the line-charging current value. For differential elements responding to the phase currents, this sensitivity limitation affects the relay fault resistance coverage for internal faults. The negative- or zero-sequence components of the charging current are very low compared to the positive-sequence or phase values. Set a negative-sequence or a zero-sequence differential element to be much more sensitive than a phase element.

Channel Time-Delay Compensation Errors

Communications channel time delay produces an apparent phase shift between the local current and the received remote current in current-only pilot protection systems. The most widely used solution is to estimate/ measure and compensate for the channel time delay.

Digital line differential protection systems typically use independent (nonsynchronized) sampling clocks and align the computed phasors. The universal technique to align the phasors, known as the ping-pong technique, involves measuring the time delay between the sampling pulses at two different locations. Once the delay between the two sampling pulses is measured, the two phasors corresponding to these two sampling pulses are time aligned.

The ping-pong technique assumes equal delay or symmetry in the communications channel. In some channels the transmit path has a different propagation delay from the receive path. This asymmetrical communications delay can exist, for example, on digital communications networks employing SONET self-healing-ring technology. The level of asymmetry depends on the

architecture of the communications system. The delay differences are typically 1 to 2 ms. Delays of 3 to 5 ms are rare and only exist on systems with fiber lengths greater than 100 miles and with 20 or more nodes in the ring.

Communications channel asymmetries generate an error in the time alignment of phasors $\vec{I}_L$ and $\vec{I}_R$. Figure 8 shows the effect of this error in the current-ratio plane. Note that channel asymmetry expands the ideal fault and load regions in Figure 5. Thus, the greater the channel asymmetry, the higher you must set the slope to ensure security: higher slopes mean reduced sensitivity.

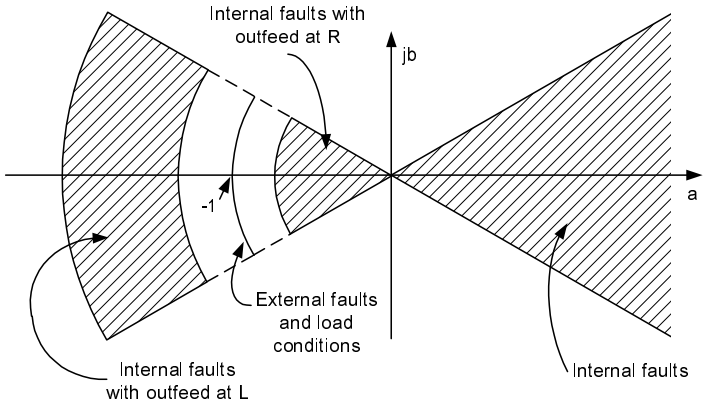

Figure 8 Effect of the Channel Time-delay Compensation Errors

A NEW DIFFERENTIAL ELEMENT FOR LINE PROTECTION

The key factors to consider in defining the required shape of a line differential relay characteristic in the current-ratio plane are channel time-delay compensation errors, power system impedance non-homogeneity, CT saturation, and low frequency oscillations in series-compensated lines. We can use negative- or zero-sequence currents to virtually eliminate the effect of line charging current and the system power angle. We also have design solutions to address the tapped load problem. Therefore, it is not necessary to consider these three factors to define the shape of the relay characteristic.

Channel time-delay compensation errors create a rotation of the ideal fault and load regions in the current-ratio plane (see Figure 8). The angle of that rotation equals the error in angle θ created by channel asymmetry. System impedance nonhomogeneity produces a rotation of the ideal internal fault region in the current-ratio plane (see Figure 6). In a worst-case scenario, these angle errors add to that produced by channel asymmetry. Figure 9 shows the combined effect of channel asymmetry and system impedance nonhomogeneity.

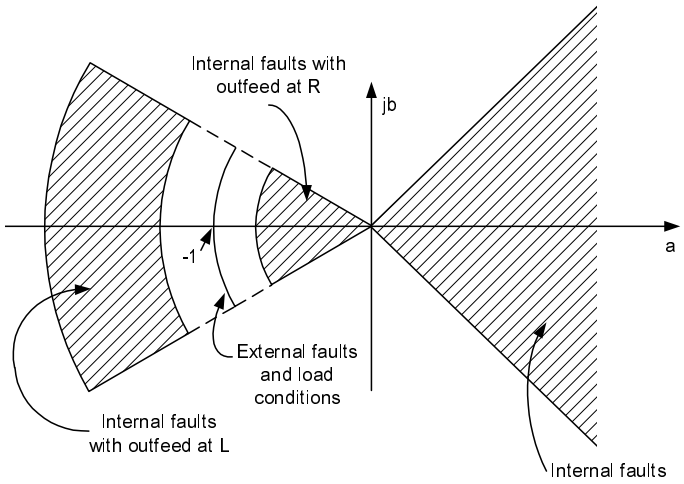

Figure 9 Combined Affect of Channel Asymmetry and System Impedance Non-Homogeneity

Figure 10 shows the characteristic of a new differential element for transmission line protection. The relay restraining region in the current-ratio plane is the area between two circle arcs and two straight lines and includes a = –1. We may create this characteristic by combining amplitude and phase comparison. Amplitude comparison provides the circular parts of the characteristic. Phase comparison provides the linear parts of the characteristic and defines the angular setting. Note that we can set the characteristic to match perfectly with the different fault and load regions shown in Figure 10 and yet accommodate CT saturation and low-frequency oscillation effects in series-compensated lines. The characteristic is symmetrical with respect to the a-axis, and the radii of both arcs are reciprocal.

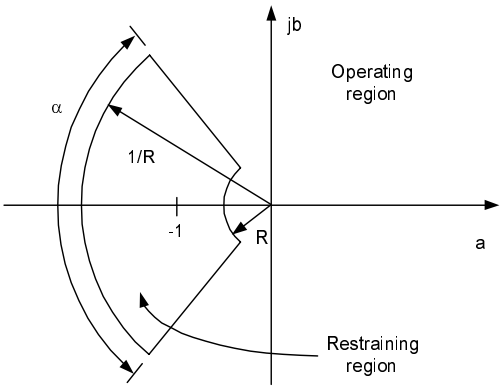

Figure 10 Characteristic of the New Differential Element in the Current-Ratio Plane

Figure 11 presents a comparison between the new characteristic and that of a traditional differential element (we assume a circular characteristic for simplicity). When we set both relays for the same level of tolerance to outfeed (Figure 11(a)), the traditional differential relay has very low tolerance to channel asymmetry. If we increase the slope of the traditional relay to accommodate a high level of channel asymmetry (Figure 11(b)), the relay loses sensitivity to internal faults with outfeed.

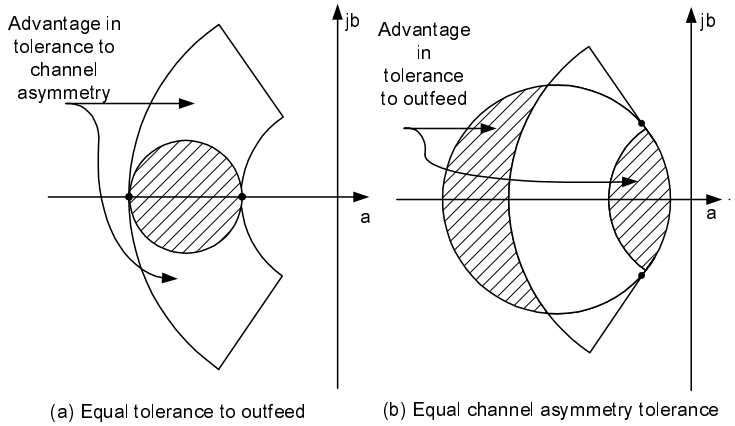

Figure 11 Advantages of the New Characteristic Over the Traditional Differential Characteristic

COMPARING GROUND FAULT SENSITIVITIES

Let us next review how much ground fault resistance directional, distance, and traditional 87L elements, and the new alpha-plane differential elements can sense on the example system shown in Figure 12. To illustrate a worst-case example, we include load flow of 4.9 A from left to right. The A-phase ground fault location shown in Figure 12 is on the line-side of the breaker associated with Relay L.

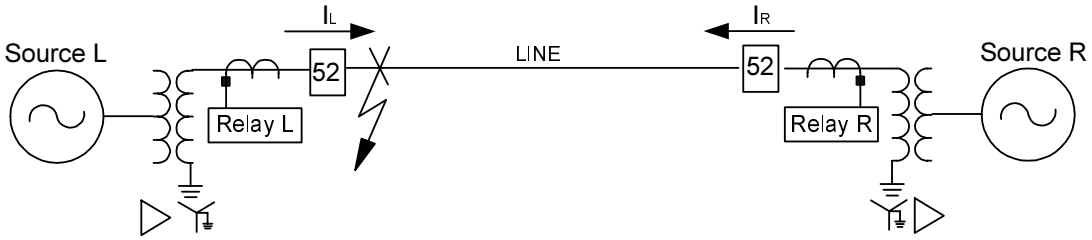

	Source L	Line	Source R
Positive-Sequence:	1Ω ∠90°	5.0Ω ∠84.3°	1Ω ∠90°
Zero-Sequence:	1Ω ∠90°	15.0Ω ∠84.3°	1Ω ∠90°

Figure 12 Example System Single-Line Diagram for Sensitivity Study

Table 2 presents the maximum settings allowed for each type of protective element to just detect the internal fault for the fault resistance values listed. All of the protective elements sense low-impedance faults very well while being very secure. To detect the internal fault as fault resistance increases, we must expand the alpha plane coverage for the new 87L element, decrease the slope of the traditional 87L, increase the reach of the mho ground distance, and increase the resistive reach of the quadrilateral element.

In a practical application, we should limit the inner and outer alpha-plane radii to 0.25 and 4 respectively to allow for some degree of CT saturation. Thus, the sensitivity of the phase alpha-plane 87L element is limited to $5 < R_F < 10\ \Omega$. Notice however that the negative-sequence alpha-plane 87L element operates to trip until 125 Ω secondary (where the element becomes blocked by a supervisory ratio of $|I2|/|I1| > 0.03$. For the traditional phase 87L element, we must decrease the slope to sense the higher impedance ground faults. This decreasing slope makes the element less secure to CT saturation and communications channel asymmetry.

Looking now at the distance elements shown in Table 2, we see that we must increase the reach as R_F increases. Assuming a three percent cumulative error in the VTs and CTs, we must limit the resistive reach of the quadrilateral element to approximately 40 Ω ([29], [33]). Thus, the quadrilateral element can reliably and securely sense up to 35 Ω secondary. For the mho ground distance element, its reach is limited by the supervisory negative-sequence directional element (we do not concern ourselves with how much overreach this element has in a pilot-scheme application). This directional element [29] has an R_F limit of 35 Ω secondary in this application for a line-asymmetry generated unbalance of 10 percent.

Table 2 Comparison of Sensitivity Limitations of Differential, Directional, and Distance Elements

R_F	Alpha Plane		Min. Distance Element Reach [Ω sec.]			Traditional 87L
[Ω sec.]	I_{AR}/I_{AS}	I_{2R}/I_{2L}	Mho	Quadrilateral Reactive	Quadrilateral Resistive	Max. Slope [%]
0	0.13∠-32°	0.17∠5°	0.00	0.0	0.0	100
1	0.06∠-60°	"	0.66	"	1.1	100
2	0.06∠-139°	"	2.31	"	2.2	90
3	0.11∠-167°	"	4.55	"	3.3	82
5	0.21∠-178°	"	9.75	"	5.5	65
10	0.39∠-178°	"	21.82	"	11.1	44
15	0.50∠178°	"	30.40	"	16.6	33
20	0.58∠178°	"	36.30	"	22.2	27
35	0.74∠178°	"	45.85	"	40.1	14
125	0.90∠178°	"	57.33	"	138.7	5

Current Transformer Saturation

CT saturation during external faults produces false operating current in a differential protection scheme. To avoid relay misoperation, desensitize the traditional 87L relay by selecting the appropriately higher value of the slope, K. Recall that increasing K increases the alpha-plane area covered by the restraint characteristic. The larger the area covered, the less R_F coverage afforded. We use the current-ratio plane to visualize the effect of CT saturation and to determine the relay settings.

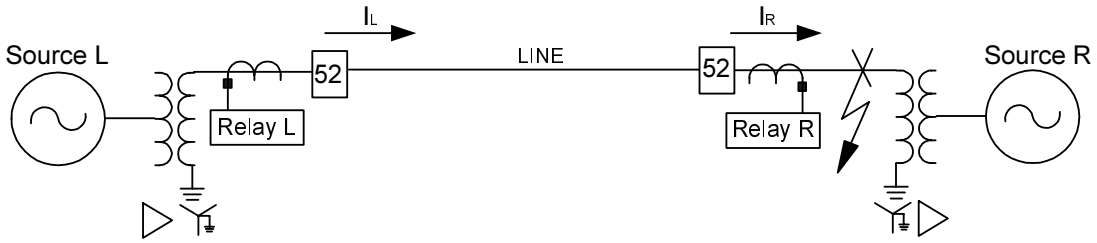

	Relay @ L	Relay @ R
Ratio and ANSI Class:	400:1 (C800)	400:1 (C400)
CT Burden (rated):	1 Ω (8 Ω)	2 Ω (4 Ω)
X/R:	28 (system angle = 87.95°)	28

Figure 13 Example System Single-Line Diagram

Let us next review a CT saturation case for an out-of-section fault (see Figure 13) to illustrate how this new alpha-plane 87L element maximizes sensitivity while optimizing security. To illustrate a worst-case scenario, we purposefully mismatch the CT voltage. Such mismatches can occur when transmission lines are looped to add new mid-line substations.

For the fault shown in Figure 13, we assume that only the current transformers (CTs) associated with Relay R saturate. This situation can also be caused by remnant flux in the CT core from an earlier internal fault. Figure 14 shows the raw currents presented to the 87L scheme and resulting current magnitude at both line ends. The digital filter for this example is a one-cycle cosine filter. If the CTs connected to Relay R had not saturated, the current magnitude calculated by Relays R and L would differ only by the line charging current and communications channel errors. However, because CTs associated with Relay R do saturate, the 87L scheme is presented with a significant amount of difference current (where $I_{OP} = I_L + I_R$). Note that the ideal secondary current magnitude at both line ends for this example is 35 A secondary.

How can we quantify how much a CT saturates? Using Stan Zocholl's [32] CT saturation limit equation, we can approximate how much a CT saturates by how much it is undersized (assumes no remnant flux).

$$\frac{\left[\left(\frac{X}{R}+1\right)\cdot I_F \cdot Z_B\right]}{20} = USF$$

Using X/R = 28, $I_F = 7$, and $Z_B = 0.5$ results in an Under Size Factor (USF) of 5 (where ideally USF ≤ 1). This means that for the given voltage class, fault current, and burden the CT must be over five times larger to completely avoid saturation. Simply increasing the voltage class to C800 reduces the USF to a tolerable 1.27.

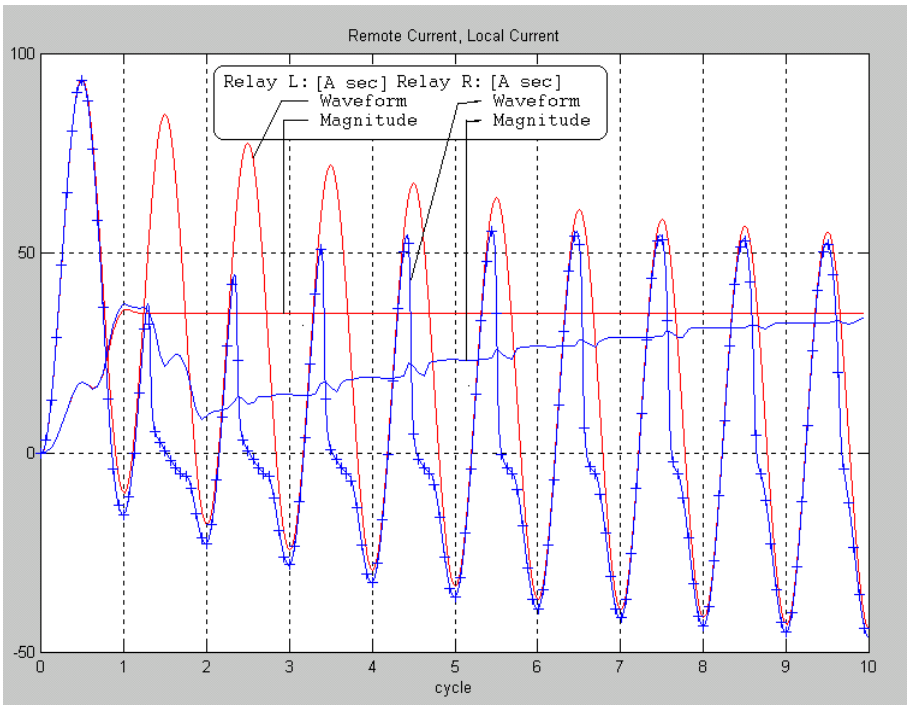

Figure 14 Raw Phase Currents and Filtered Current Magnitudes for Out-of-Section Fault

The plot shown in Figure 15 shows the results of the two different yet secure line differential protection schemes for the out-of-section fault described above. The numbered dots connected by a solid line represent the calculated alpha-plane results progressing in time. To obtain this figure, we calculated the fundamental phasor values of currents $\vec{I}_L$ and $\vec{I}_R$, using the output signals of the 16 samples-per-cycle cosine filters. We then determined the phasor $\vec{I}_R / \vec{I}_L$ ratio and plotted the result on the complex plane. We should select a slope value in the differential relay such that the relay characteristic encloses all the cluster of points where the difference current is above the minimum value. Notice in Figure 15 that the alpha-plane restraint region covers less area along the negative real axis than does the traditional slope methodology, yet both methods achieve the same security for CT saturation. Not covering this area in the alpha plane gives the phase 87L element more ground fault sensitivity during heavy load flow periods.

Once a CT saturates during an out-of-section fault, it does not immediately recover from this saturation when the external fault is cleared. Hence, if one terminal CT was saturated for an out-of-section fault while the other terminal CTs did not saturate, and the line is carrying load current, the differential relay can measure an operate current until the saturated CT recovers. Given sufficient operate or enabling current, a differential relay may operate shortly after the external fault is cleared. To address this possible misoperation condition, the 87L relay must include security logic to block element operation for a short time after the relay detects an out-of-section fault. If the relay does not have this logic, you must desensitize the relay.

Directional Element Performance During CT Saturation

We can also represent the new alpha-plane 87L element using two amplitude comparators to form the arc, and a current-only directional element shown in Equation 17. The bottom plot of Figure 15 shows the output calculations from the directional element calculation shown in

Equation (17) for an out-of-section ground fault. Negative results indicate a reverse fault direction declaration.

$$\mathrm{Re}\left(I_L \bullet I_R *\right) \tag{17}$$

where:

Re = Real operator, * = Complex conjugate operator

Notice that the directional element correctly declares the fault direction as reverse. As the left terminal CT saturation reduces, the directional element calculation desirably becomes more negative.

The middle plot of Figure 16 shows the phase angle error caused by the Terminal R CT saturation. Notice that this error is lagging: CT saturation causes the secondary current to become more leading. The maximum tolerable error is 90 degrees. If the angle error reaches 90 degrees, the directional element has zero torque. If the angle exceeds 90 degrees, the directional element makes an incorrect declaration.

Negative-sequence elements are more secure than zero-sequence 87L elements during CT saturation. To understand this point, we first recall that CT saturation causes a reduction in CT secondary current magnitude while also causing the secondary current to become more leading. Figure 17 illustrates the basics of why negative-sequence is more secure for an out-of-section A-phase fault where only one line terminal CT saturates. From this figure, notice that with zero-sequence, the two nonfaulted phase currents are unaffected. Adding the B- and C-phase current vectors to a reduced, and more leading, A-phase current results in a zero-sequence current reversal. From Figure 17 also note that negative-sequence current does not experience the same reversal. Incoming load flow aggravates this zero-sequence current reversal.

Series-Compensated Lines

Series-compensated line protection is one of the most difficult tasks for protection engineers [24], [25], [26], [27]. Series capacitors introduce a capacitive reactance that changes the typical inductive behavior of the power system for some fault types and fault locations.

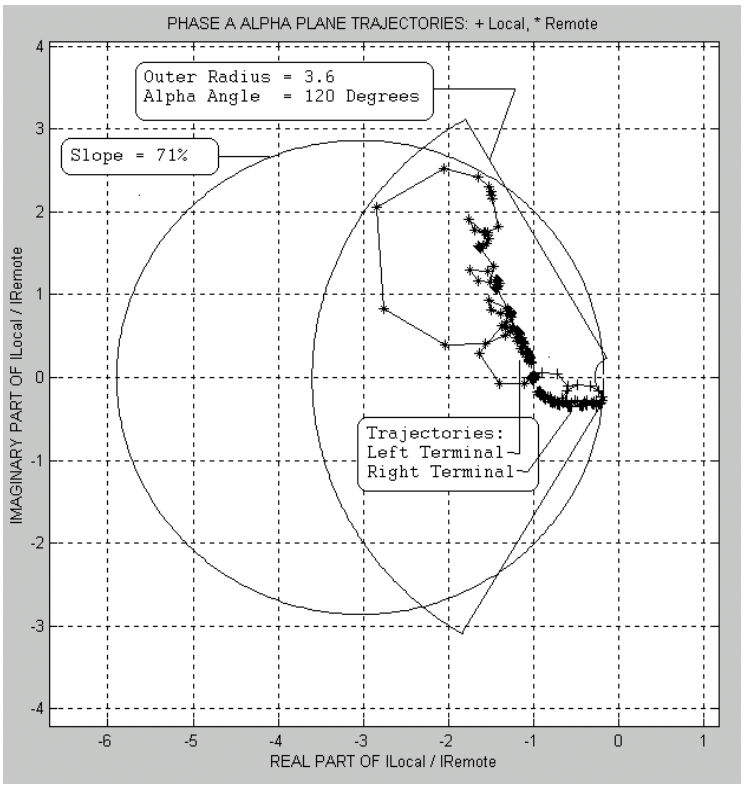

Figure 15 Alpha Plane Differential Element Gives Same Security for External Faults While Permitting Higher Sensitivity than Slope Characteristic Differential Element for Internal Faults

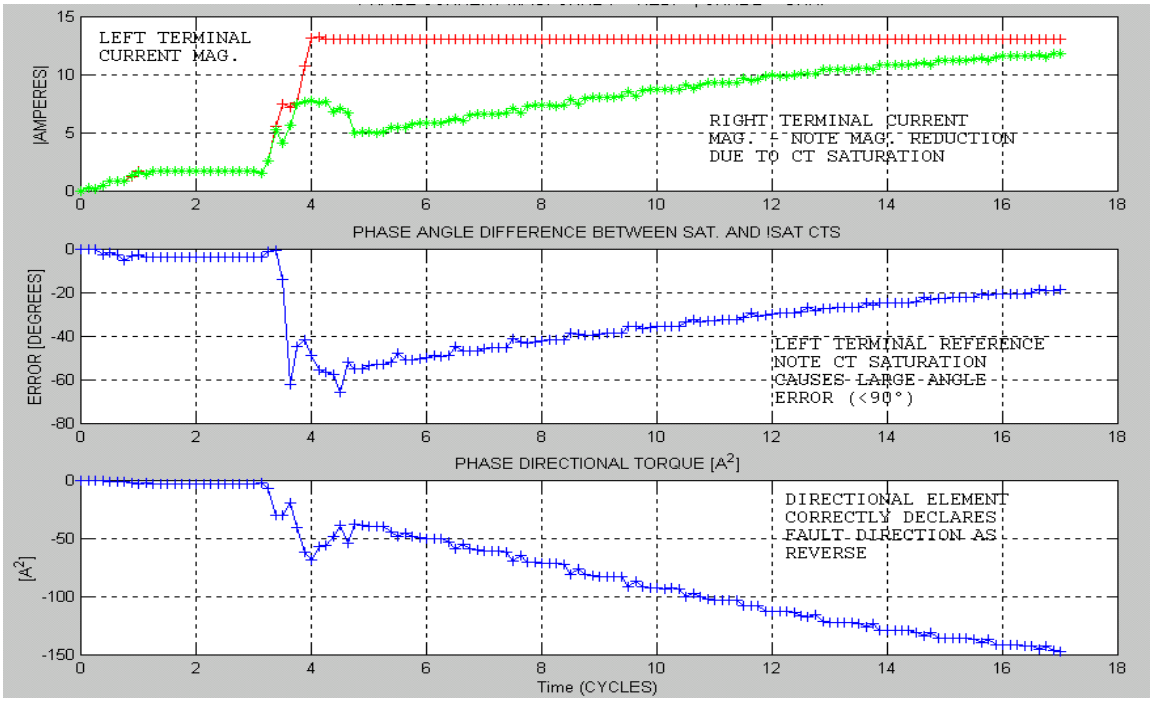

Figure 16 Directional Element Security is Tolerant of CT-Saturation-Caused Magnitude and Angle Errors

Typical steady-state problems caused by the series capacitors are voltage reversals, current reversals, and distance relay reach errors. A voltage reversal occurs for a fault near a series capacitor when the impedance from the relay voltage measuring point to the fault is capacitive. As a result, the relay voltage is shifted approximately 180 degrees from its normal position in an inductive system. Voltage inversion causes a directional relay to declare a forward fault on the protected line as reverse after the polarizing voltage memory is corrupted for a three-phase fault. A current reversal occurs when the net reactance from one of the sources to the fault point is capacitive. As a result, the current appears to be entering at one end of the line and leaving at the other for an internal fault (outfeed condition).

Current reversals may affect the operation of current-only protection systems. The presence of the series capacitor between the relay voltage measuring point and the fault point also affects the reach estimation of distance relays.

Series capacitors also introduce transient effects in the power system. One of these problems is the decaying low-frequency oscillation from the LC circuit formed by the capacitor and the system inductance. This causes the distance relay impedance estimate of a distance relay to oscillate. As a result, the relay may over- or underreach or have directional discrimination problems. We use the current-ratio plane to visualize the effect of low-frequency oscillations on current-only systems.

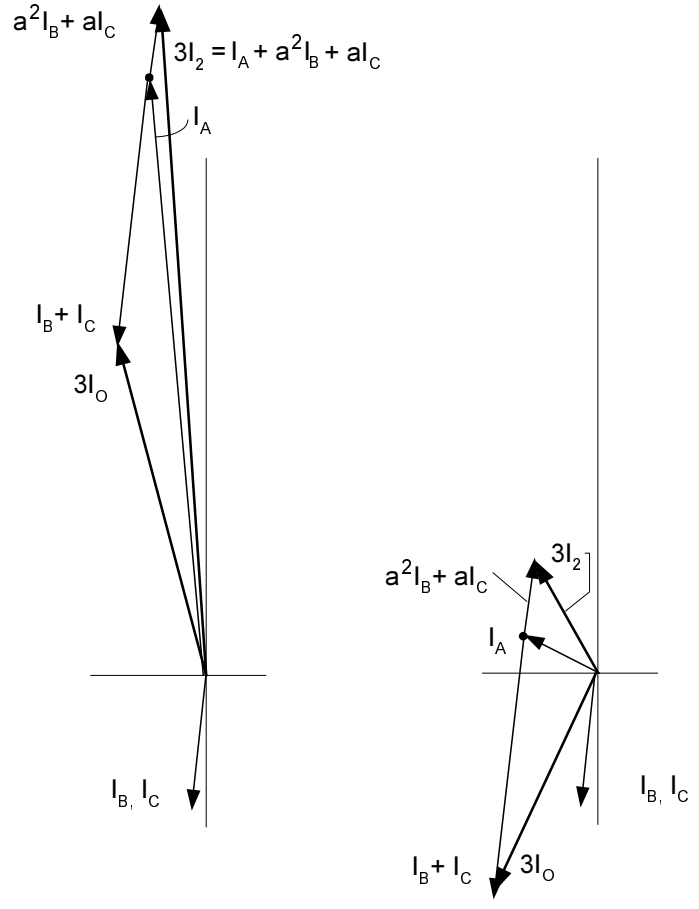

Figure 17 Zero-Sequence Current Experiences Reversal Caused by CT Saturation

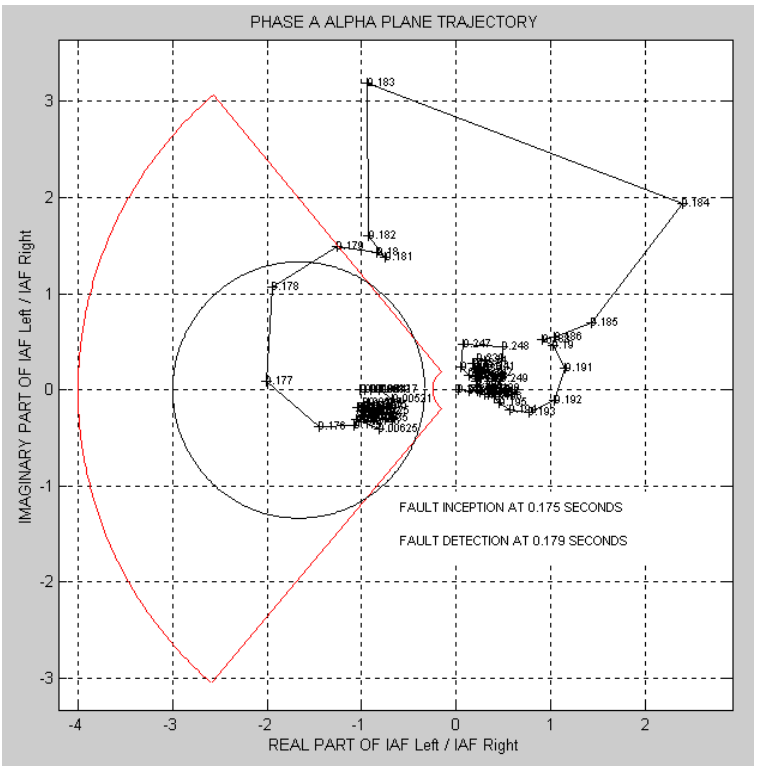

Figure 18 Effect of the Series Capacitor

Figure 18 shows a typical current-ratio trajectory for an internal fault in the series-compensated line. Note that the ratio trajectory proceeds from the left- to the right-half semi-plane after fault inception, but that some points during the transient state remain close to the b axis. Restricting the restraint region alpha angle (α) to 100 degrees allows faster tripping. The consequence of this faster operating time is that the channel asymmetry and allowable CT saturation limits must be much less than that for α = 180 degrees. These restrictions are not severe for series-compensated lines where the importance of the line warrants better CTs, an increase in communications channel routing attention, and operating instructions to the communications company.

DIRECTIONAL ELEMENT TOLERANCE TO COMMUNICATIONS CHANNEL ASYMMETRY

Ideally, the communications channel delay between terminals is equal among all line ends. However, in unidirectional SONET systems this is not always reality. The directional element represented by Equation (18) is a current only element using negative-sequence currents (balanced faults use positive-sequence quantities):

$$T32Q = \mathrm{Re}\left(I_{A2S} \bullet I_{A2R}\,^{*}\right) \tag{18}$$

where:

T32Q = Torque-like quantity compared against forward and reverse thresholds.
I_{A2S} = Negative-sequence current measured at the S-Terminal
I_{A2R} = Negative-sequence current measured at the R-Terminal
Re = Real operator
* = Complex conjugate operator

The result of Equation 18 must exceed a positive threshold to declare a forward fault direction. We can also represent Equation 18 in the familiar trigonometric form as:

$$T32Q = \left|I_{A2S}\right| \bullet \left|I_{A2R}\right| \bullet \cos\left(\theta_S - \left(\theta_R + T\right)\right)$$

where:

θ_S = Angle of I_{A2S}
θ_R = Angle of I_{A2R}
T = Error angle introduced by asymmetrical channel delay

For an external fault without CT saturation, the limit of T is ±90 degrees. This is the equivalent threshold for α = 180 degrees of the new differential element shown in Figure 11. In an 87L application, T is not simply 4.167 ms. of asymmetrical delay if the relay uses the average channel delay (commonly referred to as the ping-ping timing method). If we consider the use of the average channel delay, how much asymmetrical channel delay can the directional element tolerate? The following equation represents the equations necessary to calculate the maximum channel asymmetrical delay for an external fault.

$$T_{MAX,DEG@S} = \frac{360°}{16.67\text{m sec}} \bullet \left[\left(\frac{ts + tr}{2}\right) - ts\right] ms =$$
$$\frac{360°}{16.67\text{m sec}} \bullet \frac{[tr - ts]}{2} ms = 90°$$

where:

ts = channel delay from Terminal S to Terminal R
tr = channel delay from Terminal R to Terminal S

Solving for (tr – ts) results in $T_{MAX,DEG@S}$ = 8.33 ms. This value is a significant amount of channel asymmetry delay tolerance. Directional elements must also tolerate the phase angle delay introduced by CT saturation. Thus, the directional element must tolerate the combined angle errors of CT saturation and channel delay asymmetry as a worst-case scenario. If the resulting angle error from channel asymmetry and CT saturation exceeds ±90 degrees, the directional element makes the incorrect declaration. You can make a similar observation about the new alpha-plane 87L element. For a directional comparison scheme, we can substitute V_{A2S} for I_{A2R}, set T = 0, and reach the same conclusion: that this type of directional element can tolerate up to 90 degrees of angle error from CT saturation.

THREE-TERMINAL LINE CT SATURATION FOR EXTERNAL FAULT SECURITY LOGIC

Figure 19 shows a parallel line, three-terminal application. Each line operates most of the time with all three breakers closed but may be transformed to a two-terminal line at any time by the opening of a breaker. Thus, any three-terminal logic must also be applicable for two-terminal applications.

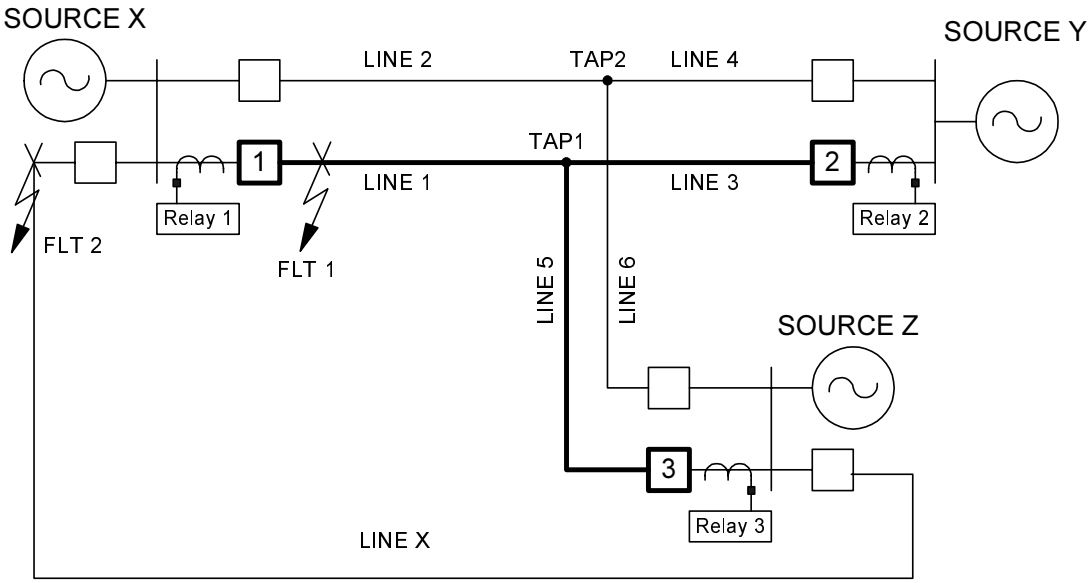

Figure 19 Typical Three-Terminal Line Single-Line Diagram

For the system shown in Figure 19, the directional comparison and 87L schemes must operate for any fault on Line Sections 1, 3, or 5 with one or two breakers open.

Three-Terminal Line Application Complications

The primary complication for these applications is "out-flow" at one of the three terminals for an in-section fault close to one of the other terminals. For example, with a fault location such as that shown as FLT 1 in Figure 19, current may flow into the bus on Line Section 5 if the impedance of Line 5 plus Line X is less than that of Line Section 1. Current flowing into a line terminal for an in-section fault is called out-flow. Note that the direction of current flow through Breaker 3 for FLT 1 is the same direction as that for FLT 2 (for which the 87L element for the line shown in bold must restrain).

In a directional-comparison scheme, the outflow at Breaker 3 causes Relay 3 to declare a reverse-fault direction. This singular reverse fault declaration defeats high-speed tripping by the directional comparison scheme.

Similarly, outflow at Breaker 3 defeats many 87L elements (e.g., segregated phase comparison). One effective 87L scheme converts the three-terminal line into a two-terminal line. With this logic, this new 87L element can reliably detect in-section faults while restraining for external faults with one, two, or all breakers closed. This means that you cannot simply compare the

direction of current at a single measuring terminal with that received from the other two terminals to determine if the fault is in- or out-of-section.

New Three-Terminal Directional Element Scheme

The logic shown in Figure 20 overcomes the outflow complication described above. Each relay, in a three-step rotation, combines two of the currents from three terminals and treats the resulting current as the remote current. The remaining terminal current is treated as the local current. After repeating this process three times, each relay compares the results. For internal faults without outflow, none of the three 87L calculations indicates restrain. Given sufficient operate current the 87L operates to trip. If one terminal has outflow, at least one of the three 87L calculations will indicate trip.

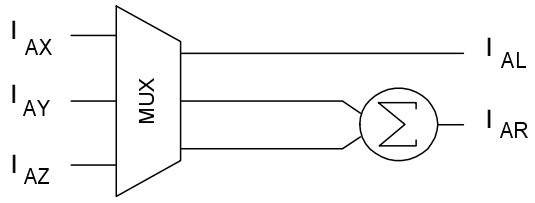

Figure 20 General Logic for Converting Three-Terminal Analogs to Two-Terminal

Table 3 shows the current flow directions of the faulted phase currents at each terminal for faults located at FLT 1 and FLT 2. Let us review an outflow case from Table 3, given an in-section fault located at FLT 1 with Line X and all sources in-service, Relays X and Y measure current from the bus to the line (indicated by the → symbol in Column 4). In our example, we assume that the impedance of Line X + Line 5 is less than that of Line 1. With Line X in service, Relay Z senses current into its terminal (indicated by the ← symbol). The vector sum of Relay Y and Z currents is dominated by the Relay Y current. This causes the remote terminal current, I_R (see Column 5), to be in the same direction as the current measured by Relay X. Thus, the 87L decision using Relay X current as the local current is in the trip region. Using Relay Y current as the local current also results in a trip decision. However, using Relay Z as the local current for the 87L logic results in a restrain decision. Since we can only have outflow at one terminal, we recognize this combination of trip and restrain conditions in the absence of CT saturation as an in-section fault.

Table 3 Current Flow Directions for Faults FLT 1 and 2 in Figure 19

1	2			3	4	5		6	7
Flt @	**Source X**	**Y**	**Z**	**Line X**	**Local Terminal, I_{2L}**	**Remote Terminal (I_{2R}) Combination**		**Section Declaration**	**Trip or Restrain**
1	IN	IN	IN	OUT	$I_L = X \rightarrow$ $I_L = Y \rightarrow$ $I_L = Z \rightarrow$	$Y\rightarrow + Z\rightarrow$ $X\rightarrow + Z\rightarrow$ $X\rightarrow + Y\rightarrow$	$I_R\rightarrow$ $I_R\rightarrow$ $I_R\rightarrow$	$\rightarrow \bullet \rightarrow = IN_X$ $\rightarrow \bullet \rightarrow = IN_Y$ $\rightarrow \bullet \rightarrow = IN_Z$	TRIP
"	IN	IN	IN	IN	$I_L = X \rightarrow$ $I_L = Y \rightarrow$ $I_L = Z \leftarrow$	$Y\rightarrow + Z\leftarrow$ $X\rightarrow + Z\leftarrow$ $X\rightarrow + Y\rightarrow$	$I_R\rightarrow$ $I_R\rightarrow$ $I_R\rightarrow$	$\rightarrow \bullet \rightarrow = IN_X$ $\leftarrow \bullet \rightarrow = IN_Y$ $\rightarrow \bullet \rightarrow = OUT_Z$	TRIP (no sat.)
"	OUT	OUT	IN	IN	$I_L = X \rightarrow$ $I_L = Y \leftarrow$ $I_L = Z \rightarrow$	$Y\leftarrow + Z\rightarrow$ $X\rightarrow + Z\rightarrow$ $X\rightarrow + Y\leftarrow$	$I_R\rightarrow$ $I_R\rightarrow$ $I_R\rightarrow$[1]	$\rightarrow \bullet \rightarrow = IN_X$ $\leftarrow \bullet \rightarrow = OUT_Y$ $\rightarrow \bullet \rightarrow = IN_Z$	TRIP (no sat.)
2	IN	IN	IN	OUT	$I_L = X \leftarrow$ $I_L = Y \rightarrow$ $I_L = Z \rightarrow$	$Y\leftarrow + Z\leftarrow$ $X\leftarrow + Z\rightarrow$ $X\leftarrow + Y\rightarrow$	$I_R\rightarrow$ $I_R\leftarrow$ $I_R\leftarrow$	$\leftarrow \bullet \rightarrow = OUT_X$ $\rightarrow \bullet \leftarrow = OUT_Y$ $\rightarrow \bullet \leftarrow = OUT_Z$	No TRIP
"	OUT	OUT	IN	IN	$I_L = X \leftarrow$ $I_L = 0$ $I_L = Z \rightarrow$	$Y\leftarrow + Z\rightarrow$ $X\leftarrow + Z\rightarrow$ $X\leftarrow + Y\leftarrow$	$I_R\rightarrow$ $I_R\rightarrow$ $I_R\leftarrow$	$\leftarrow \bullet \rightarrow = OUT_X$ $\leftarrow \bullet \rightarrow = OUT_Y$ $\rightarrow \bullet \leftarrow = OUT_Z$	No TRIP
"	OUT	IN	OUT	IN	$I_L = X \leftarrow$ $I_L = Y \rightarrow$ $I_L = Z\ (0)$	$Y\rightarrow + Z\ (0)$ $X\leftarrow + Z\ (0)$ $X\leftarrow + Y\rightarrow$	$I_R\rightarrow$ $I_R\leftarrow$ $I_R\leftarrow$[1]	$\leftarrow \bullet \rightarrow = OUT_X$ $\rightarrow \bullet \leftarrow = OUT_Y$ $0 \bullet \leftarrow =$ No OP	No TRIP

Note 1: Special Case, IX = IR $\therefore I_R = 0$ assumes $\rightarrow$ direction

Let us now consider CT saturation for an A-phase fault located on Bus X, all sources in and Line X out. For discussion, let us assign the following values to the A-phase current magnitudes at each terminal: $I_{AX} = 3 \angle 90°$, $I_{AY} = 2 \angle -90°$, $I_{AZ} = 1 \angle -90°$. Given these values, and ignoring CT saturation, let us next calculate the ideal I_R / I_L at each terminal.

$$\alpha_X = \frac{(I_Y + I_Z)}{I_X} = \frac{2+1}{-3} = -1 \tag{19}$$

$$\alpha_Y = \frac{(I_X + I_Z)}{I_Y} = \frac{-3+1}{2} = -1 \tag{20}$$

$$\alpha_Z = \frac{(I_X + I_Y)}{I_Z} = \frac{-3+2}{1} = -1 \tag{21}$$

The X-Terminal CT is the most likely to saturate for this fault because it has the greatest magnitude of current. When a CT saturates, the secondary current magnitude decreases and its angle advances. The phasors shown in Figure 21 illustrate how this reduction in magnitude and advancement in angle has a detrimental effect on the security of the α_Z calculation (i.e. it declares a trip condition).

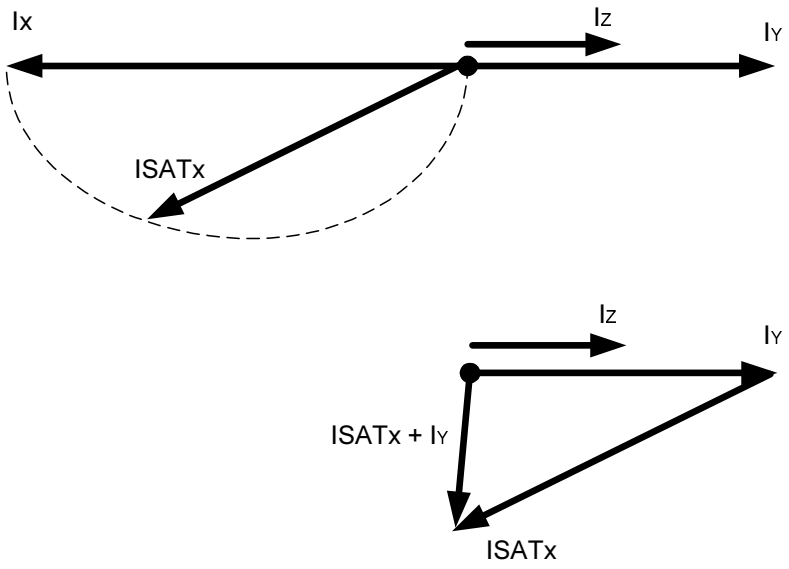

Figure 21 Phasor Diagram Showing the Effect of X-Terminal CT Saturation

Note that the ISATx current phasor magnitude in Figure 21 is less than that of the I_X current phasor. In the theoretical limit, as |ISATx| approaches zero its angle approaches 90 degrees leading from I_X. Note also that (ISATx + I_Y) in the lower phasor diagram in Figure 21 is slightly greater than –90 degrees from I_Z. Given a slightly higher degree of saturation of I_X, the angle between (ISATx + I_Y) and I_Z becomes less than 90 degrees and α_Z can declare a trip condition (depending on the settings of the restrain characteristic).

SUMMARY

1. Current-only differential schemes must balance security challenges from CT saturation and channel asymmetry with sensitivity: the more secure the scheme, the less fault coverage.

2. Factors that reduce directional-comparison scheme sensitivity are different from those that reduce 87L scheme sensitivity. Thus, directional-comparison and current-differential schemes are very complementary when we only consider sensitivity.

3. Differential relays using a slope setting cannot achieve the same sensitivity and security as an alpha-plane 87L relay when we consider the cumulative errors of CT saturation and channel asymmetry.

4. Directional elements and the new alpha-plane 87L element are very tolerant of CT saturation while maintaining a maximum degree of fault resistance coverage.

5. Using Stan Zocholl's CT sizing equation, we create a new factor called Undersized Factor: USF. If an application has a USF of 4 or less, we can securely apply the new alpha-plane 87L element.

6. Negative-sequence directional and differential elements are more secure than zero-sequence elements under CT saturation conditions.

7. Current Ratio Plane characteristic evaluation of differential elements is a simple means of analyzing the sensitivity and security of differential and current-only directional elements.

8. Restricting phase differential elements to detecting three-phase faults, while using a negative-sequence differential element to detect all other fault types, maximizes sensitivity while maintaining security.

9. For differential relaying, converting three-terminal line applications to combinations of two-terminal equivalents minimizes sensitivity and security degradations caused by outfeed.

REFERENCES

[1] IEEE Power System Relaying Committee Report, "Line protection design trends in the USA and Canada," IEEE Transactions on Power Delivery, Vol. 3, No 4, October 1988, pp. 1530–1535.

[2] S. C. Sun and R. E. Ray, "A current differential relay system using fiber optics communications," IEEE Trans. on Power Apparatus and Systems, Vol. PAS-102, No 2, February 1983, pp. 410–419.

[3] IEEE Power System Relaying Committee Report, "A survey of optical channels for protective relaying: Practices and experience, "IEEE Trans. on Power Delivery, Vol. 10, No 2, April 1995, pp. 647–658.

[4] F. Calero and W. A. Elmore, "Current differential and phase comparison relaying schemes," Proceedings of the 19th Annual Western Protective Relay Conference, Spokane, WA.

[5] G. R. Hoffman and W. L. Hinman, Method and Apparatus for Monitoring an AC Transmission Line, US Patent No 4939617, July 3, 1990.

[6] H. P. Sleeper, "Ratio-differential relay protection," Electrical World, October 1927, pp. 827–831.

[7] T. Monseth and P. H. Robinson, Relay Systems: Theory and Applications, New York: McGraw Hill Co., 1935.

[8] R. van C. Warrington, Protective Relays: Their Theory and Practice, Volume One, London: Chapman and Hall, 1962.

[9] A. R. van C. Warrington, Protective Relays: Their Theory and Practice, Volume Two, London: Chapman and Hall, 1969.

[10] F. Anderson and W. A. Elmore, "Overview of Series-Compensated Line Protection Philosophies," Proceedings of the 17th Annual Western Protective Relay Conference, Spokane, WA.

[11] Jeff Roberts et al., "Limits to the Sensitivity of Ground Directional and Distance Protection," Proceedings of the 50th Annual Georgia Tech Protective Relaying Conference, Atlanta, Georgia.

[12] Jeff Roberts, Armando Guzman, "Directional Element Design and Evaluation," Proceedings of the 49th Annual Georgia Tech Protective Relaying Conference, Atlanta, Georgia, May 3–6.

[13] Jeff Roberts, E.O. Schweitzer III, "Distance Element Design," Proceedings of the 46th Annual Conference for Protective Relay Engineers, Texas A&M Univ., College Station, TX, April 12–14.

[14] Stan Zocholl, Jeff Roberts, Gabriel Benmouyal, "Selecting CTs to Optimize Relay Performance," Proceedings of the 24th Annual Western Protective Relay Conf., Spokane, WA.

[15] Edmund O. Schweitzer, III, and John J. Kumm, "Statistical Comparison and Evaluation of Pilot Protection Schemes," Proceedings of the 23rd Annual Western Protective Relay Conference, Spokane, WA, October 15–17, 1996.

BIOGRAPHIES

Jeff Roberts received his BSEE from Washington State University in 1985. He worked for Pacific Gas and Electric as a System Protection Engineer for over three years. In 1988, he joined Schweitzer Engineering Laboratories, Inc. as the first Application Engineer. Later he became Application Engineering Manager. He now serves as the Research Engineering Manager. He has written many papers in the areas of distance element design, sensitivity of distance and directional elements, directional element design, and analysis of event report data. Mr. Roberts holds over twenty patents granted or pending. He is also a senior member of IEEE.

Demetrios A. Tziouvaras was born in Greece and moved to the USA in 1977. He received his B.S. and M.S. degrees in electrical engineering from the University of New Mexico and Santa Clara University, respectively. He joined the System Protection Group of Pacific Gas & Electric Co. in 1980, where he held the position of Principal Engineer and was responsible for the application of new technologies, design standards, and substation automation. He joined the SEL Research Group as a Research Engineer in 1998. He is a senior member in the Institute of Electrical and Electronic Engineers (IEEE) and a member of the Power System Relaying Committee of the Power Engineering Society of IEEE. He is a member of two subcommittees and chairman of two working groups, one on EMTP Applications to Power System Protection, and the other on Mathematical Models for Current, Voltage, and Coupling Capacitor Voltage Transformers. He has authored and co-authored numerous technical papers and taught seminars in EMTP, protective relaying, and digital relaying at the University of Illinois at Urbana-Champaign and the California Polytechnic Institute in San Luis Obispo, California. His interests include digital relay modeling, system protection, and power system transients. He has numerous patents pending.

Gabriel Benmouyal received his B.A.Sc. in Electrical Engineering and his M.A.Sc. in Control Engineering from Ecole Polytechnique, Université de Montréal, Canada in 1968 and 1970, respectively. In 1969, he joined Hydro-Québec as an instrumentation and control specialist. He worked on different projects in the field of substation control systems and dispatch centers. In 1978 he joined IREQ, where his main activity was the application of microprocessors and digital techniques to substation and generating-station control and protection systems. In 1997 he joined Schweitzer Engineering Laboratories in the position of Research Engineer. He is a registered professional engineer in the Province of Québec, an IEEE member, and has served on the Power System Relaying Committee since May 1989.

Hector J. Altuve received his BSEE from Central University of Las Villas (UCLV), Cuba, in 1969 and his PhD from Kiev Polytechnic Institute, USSR, in 1981. He served as a professor in the School of Electrical Engineering at UCLV from 1969 to 1993. Since 1993, he has been a professor in the PhD program of the Mechanical and Electrical Engineering School at Autonomous University of Nuevo Leon, in Monterrey, Mexico. He is a member of the Mexican National Research System, a senior member of IEEE, and a PES Distinguished Lecturer. He has authored and coauthored many technical papers. He was the 1999–2000 Schweitzer Visiting Professor at Washington State University.